INTEGRATING Q-LOGGING WITH SEISMIC REFRACTION, PERMEABILITY, PRE-GROUTING, TUNNEL AND CAVERN SUPPORT NEEDS, AND NUMERICAL MODELLING OF PERFORMANCE.

Nick Barton[1]

Abstract: When the 'Q-system' was launched in 1974, the name referred to rock mass classification, with focus on tunnel and cavern support selection. Since that time 'a system' has indeed been developed. The Q-system now integrates investigation geophysics, rock mass characterization, input for numerical modelling, empirical design of support, and excavation performance assessment. The Q-value has proved easy to correlate with required support capacity, relative cost and time for tunnel construction, seismic P-wave velocity, deformation modulus, cavern deformation, and in modified form with permeability. Recent research has also shown encouraging links between Q, the depth dependant deformation modulus, and the *seismic quality* Q_{seis}, which is the inverse of attenuation. There are also indications that Q has captured important elements of the cohesive and frictional strength of rock masses. The above sensitivities are most likely because Q is composed of fundamentally important parameters that were quantified by exhaustive case record analysis. The six-orders-of-magnitude range is a reflection of the potentially enormous variability of geology and structural geology. Some of the empirical relationships are illustrated with a summary of Gjøvik Olympic cavern investigations, and of the *discontinuum* modelling of performance. The paper concludes with a critical assessment of the potential shortcomings of *continuum* modelling of highly stressed excavations in intact rock, and of shallow excavations in anisotropically jointed rock.

INTRODUCTION

This lecture will be an illustrated journey through some of the useful linkages and concepts that have been absorbed into the 'Q-system' during the last ten years or so. From the outset the focus will be on sound, simple empiricism, that works because it reflects practice, that can be used because it can be remembered, and that does not require black-box software solutions. Some of the empiricism will be illustrated by reference to investigations and to empirical and numerical modelling performed at the Gjøvik Olympic cavern in Norway.

Nature varies a lot and therefore Q does too

It is appropriate to start by illustrating contrasting rock mass qualities. Figure 1 shows a core box from a project that has not been *completed* during ten years of trying. The second project may not be *started* for at least ten years. The first should already have passing high-speed trains, the other high-level nuclear waste some time in the future. They are both from the same country and may have six orders of magnitude contrast in Q-value. A second pair of examples shown in Figure 2, requires a cable car for access on the one hand, and successive boat trips to fault-blocked flooded sections of tunnel on the other.

The contrasting stiffness and strength of intact rock and wet clay is easy to visualize. One may be crushed by one and drowned in the other. There are sad and multiple examples of both in the tunnelling industry. They merit a widely different quality description, as given by the Q-value.

[1] Nick Barton & Associates, Oslo, Norway

Figure 1 The obvious contrasts of these two core boxes suggest orders of magnitude differences in quality. Quantitative descriptions of shear strength and deformation modulus vary by orders of magnitude as well. Quality descriptors like RMR or GSI that suggest different qualities of about 5 and 95 are not then as appropriate as 0.001 and 1000.

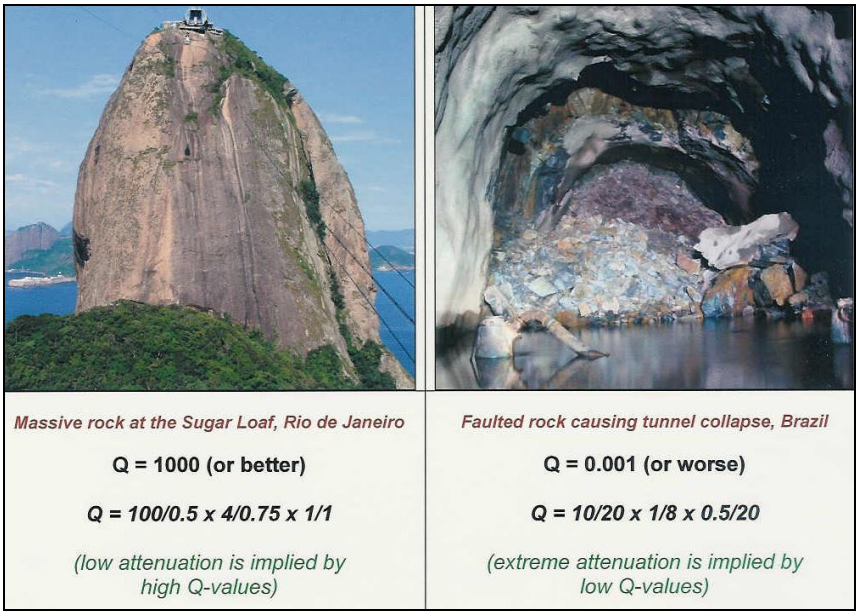

Figure 2 Respective access by cable car and by boat, emphasises the need for radically different magnitudes of ‘rock quality’, and also radically different magnitudes of ‘seismic quality’, the inverse of attenuation. Barton (2006). A single project beneath Hong Kong waters, demonstrated a ‘length’ of unjointed core of 57 m length, and an even wider regional fault zone. With such extremes, RQD values of 100% and 0% are clearly inadequate too, and can be improved by using local Q-values of, for example, 1000 and 0.001.

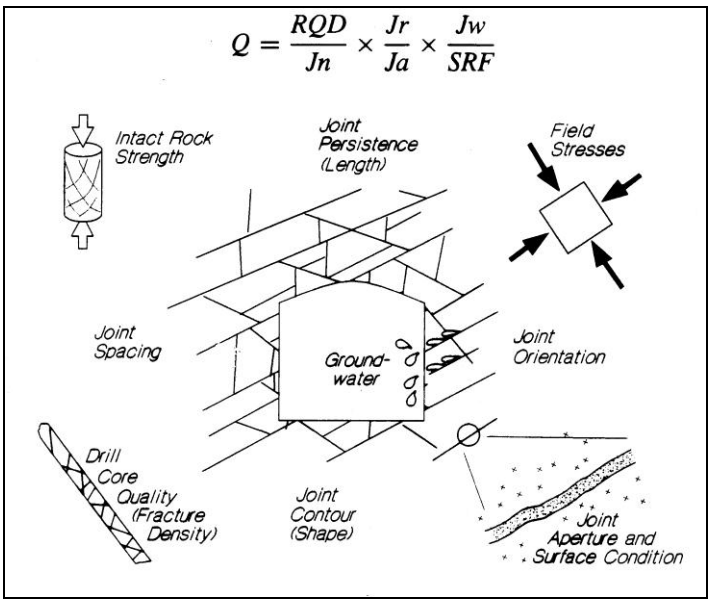

Figure 3 A pictorial impression of the sources of input data that should be captured in the Q formulation. From Hutchinson and Diedericks (1996).

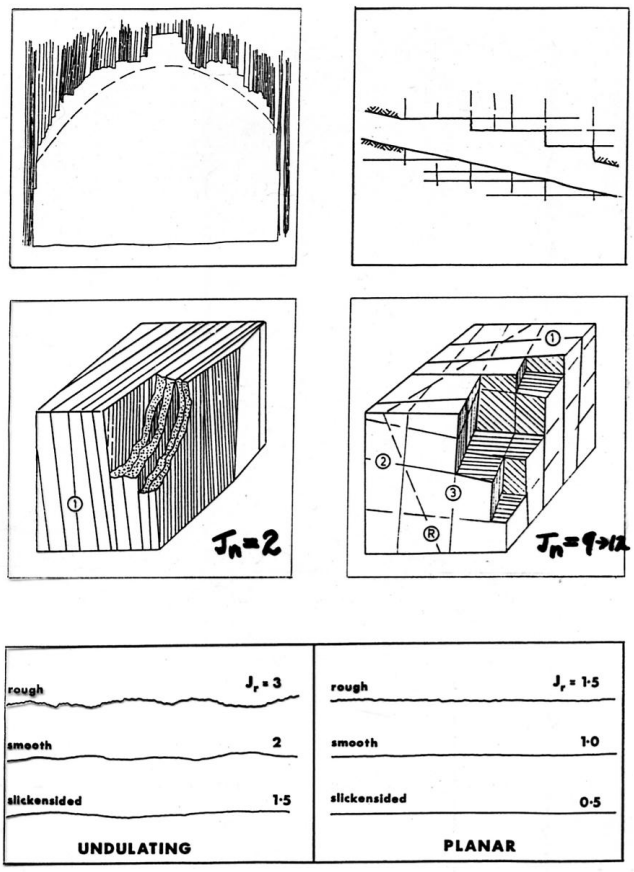

Figure 4 Two of the most important components of Q and of rock mass stability: the number of joint sets (or degree of freedom for block definition and fall-out), and the joint roughness (or inter-block release-or-hold mechanism). The general level of over-break and ease of characterization are also fundamentally affected by these two parameters.

RELATING SEISMIC ATTRIBUTES TO Q

Since there is a limit to how many boreholes can be drilled, how many cores can be logged, and how many permeability tests can be performed, it is useful to have alternative ways of estimating and extrapolating these ‘point sources’ of information.

We will start by looking at correlation between velocity and measures of quality, with Sjøgren et al. (1979) as a *very* useful starting point for the case of investigations in hard rock, using seismic profiles (totalling 120 km) and local core logging results (totalling 2.1 km of core).

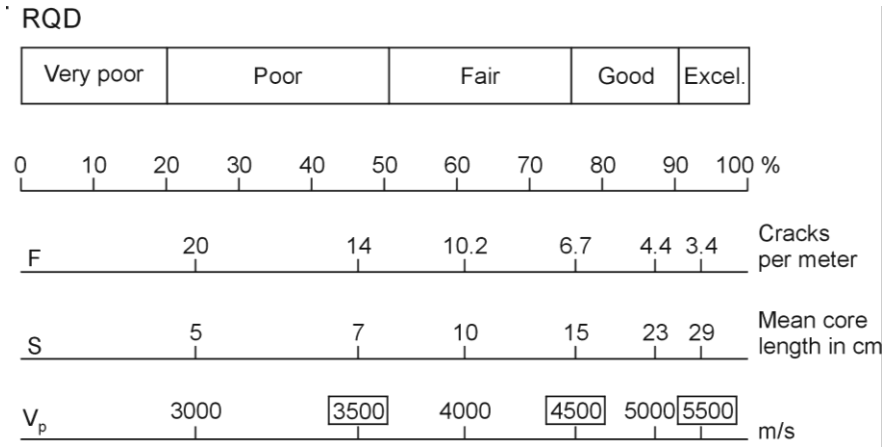

Figure 5 Hard rock, shallow refraction seismic. Sjøgren et al. (1979) combined 120 km of seismic profiles and 2.1 km of core logging to derive these mean trends.

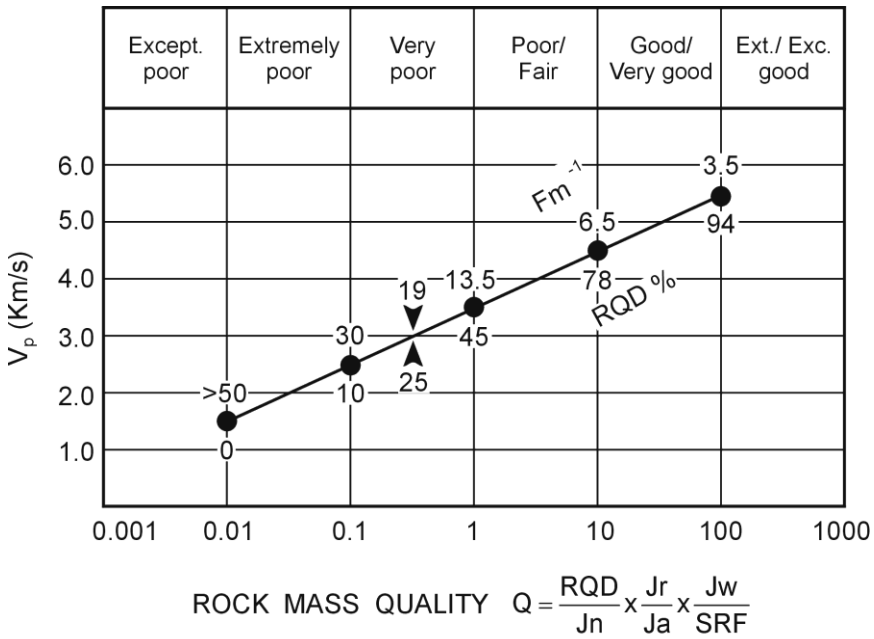

Figure 6 Hard rock, shallow seismic refraction mean trends from Sjøgren et al. (1979). The Q-scale was added by Barton (1995), using the hard rock correlation $V_p \approx 3.5 + \log Q$. By remembering Q = 1: Vp ≈ 3.5 km/s, and V_p = 3 km/s: Q ≈ 0.3, the Q-Vp approximation to a wide range of qualities is at one’s fingertips (e.g. for hard, massive rock: Q = 100: Vp ≈ 5.5 km/s, and V_p = 5 km/s: Q ≈ 30).

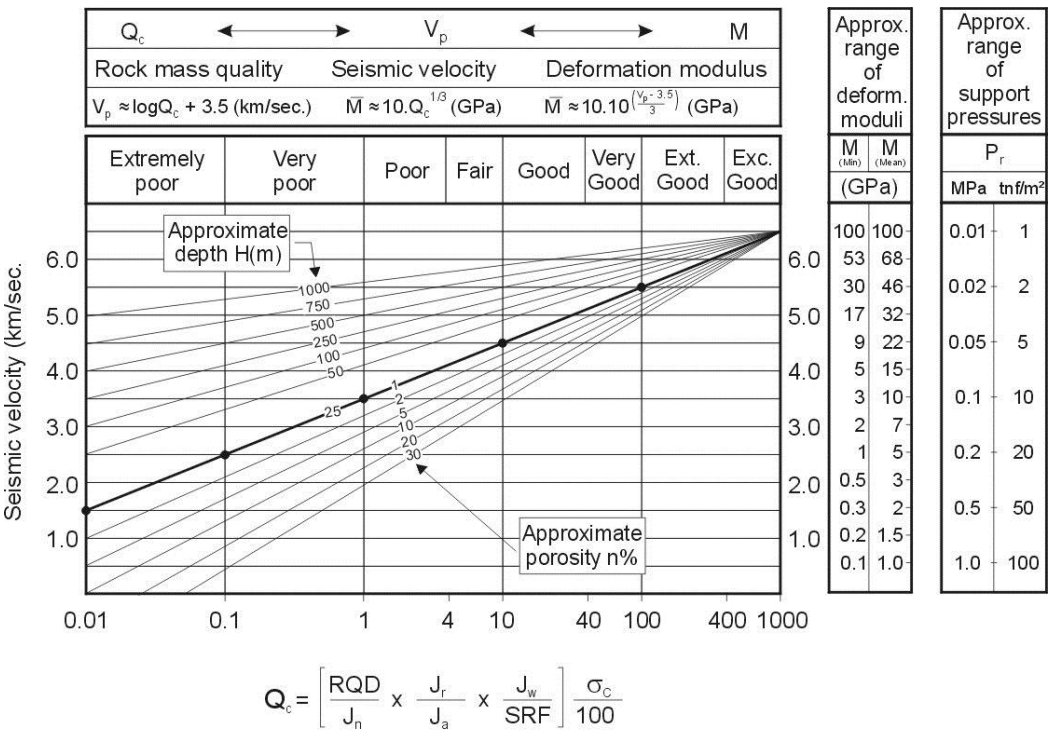

Figure 7 An integrated empirical model for linking Q-value (via Q_c) to P-wave velocity, depth, matrix porosity, deformation modulus, and approximate support pressure (based on a mean Jr = 2). With this simplification, the Barton et al. 1974 support pressure formulation, and the Barton, 1995 deformation modulus formulation suggest inverse proportionality between support pressure and deformation modulus. This is logical, but the simplicity is nevertheless surprising. Barton (2002).

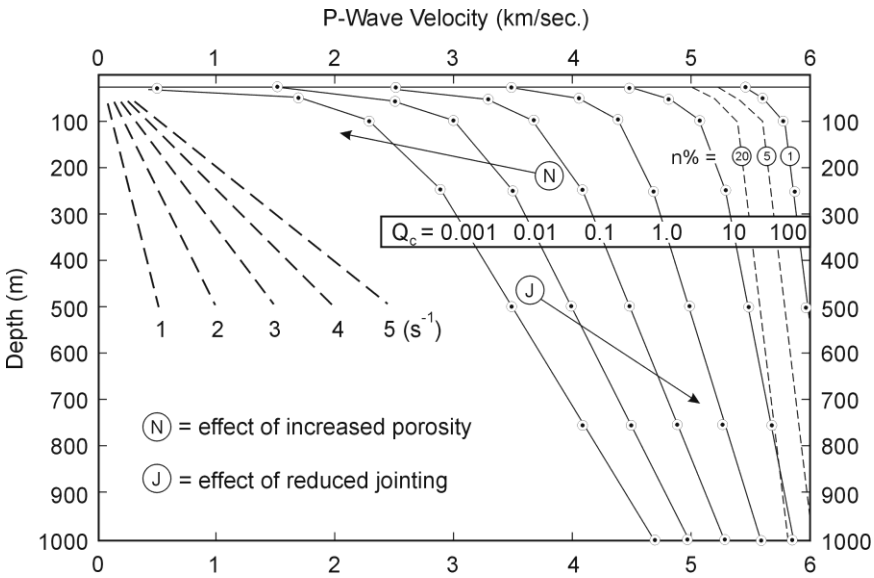

Figure 8 The depth-velocity trends for different Q_c values. This diagram explains why faulted rock ahead of a deep tunnel may sometimes be 'invisible' or of such 'high' velocity, like 4 km/s that it is misinterpreted. It may subsequently cause tunnel collapse, or trap a TBM. In fact such rock is still probably displaying an important contrast to the surrounding rock mass which also shows signs of joint closure. In the case of soft rock, acoustic closure prevents such differentiation. Barton (2006).

RELATING PERMEABILITY TO Q AND TO Q H20

Here we move into more difficult territory, since there are potential problems of flow-channels that have suffered erosion or solution-effects, and there are joints that may be clay-sealed, therefore having both low permeability *and* low Q-value.

For hard, low porosity, jointed rock masses without clay, the approximate Lugeon scales shown in Figure 9 may have some practical merit, when 'out in the field' and also away from colleagues who make a living from permeability measurements. They know best, and we need their data too.

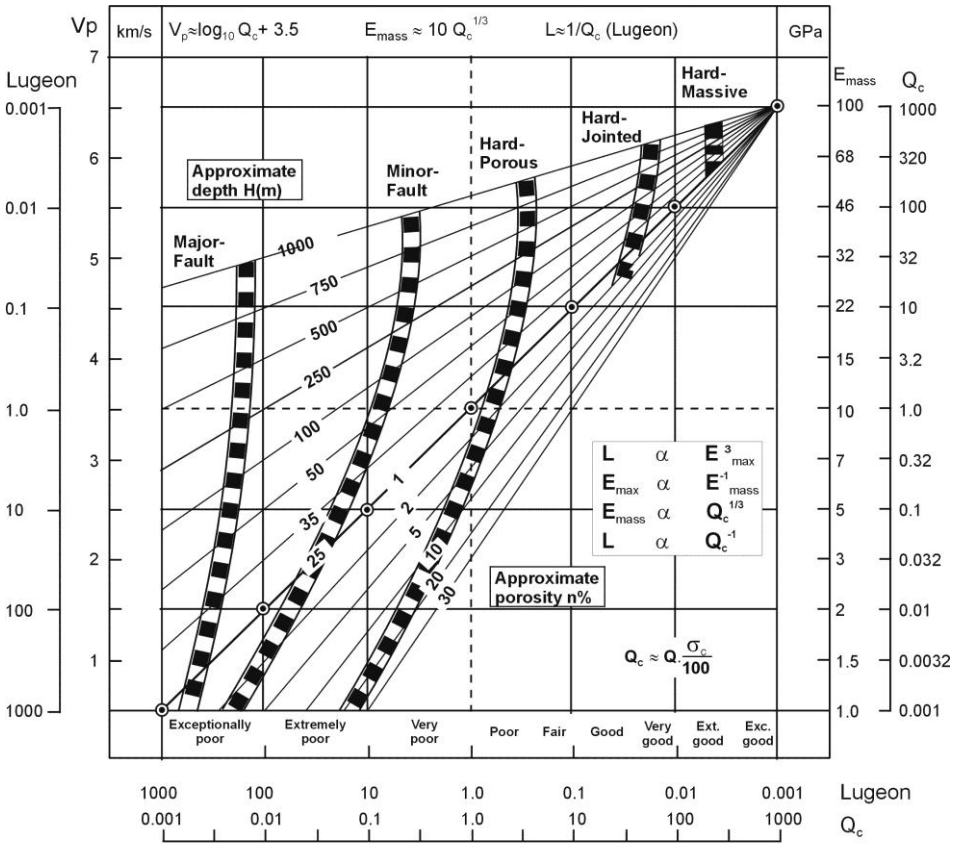

Figure 9 An extension of Figure 8 to include a very approximate estimate of Lugeon value, strictly for the case of rock masses without clay-filling (and therefore flow-blockage) of the joints. For a more general case, the modified term Q_{H2O} is used. This is shown in Figure 10. Note the 'type-curves' for e.g. 'massive rock' and 'jointed rock'. Table 1 shows a collection of potential inter-relationships, where proving them 'wrong' is also useful as anomalies may thereby be uncovered. Barton (2006).

Table 1 A set of inter-related approximations that are useful when assessing results in the field.

Q_c	0.1	1	10	100
Lugeon	10	1	0.1	0.01
K (m/s) ≈	10^{-6}	10^{-7}	10^{-8}	10^{-9}
V_p (km/s)	2.5	3.5	4.5	5.5

Table 2 The two versions of 'Q-permeability' estimation. It should not need to be emphasised that both are approximate. Both are presently based on limited test data.

$L \approx 1/Q_c$ (1 Lugeon $\approx 10^{-7}$ m/s $\approx 10^{-14}$ m^2) (hard, jointed, clay-free rock masses)	General case, with depth/stress allowance, and consideration of joint wall strength
Q_c = RQD/Jn x Jr/Ja x Jw/SRF x σ_c/100	Q_{H2O} = RQD/Jn x Ja/Jr x Jw/SRF x 100/JCS $K \approx \frac{2}{1000 \times Q_{H_2O} \times 10^{5/3}}$

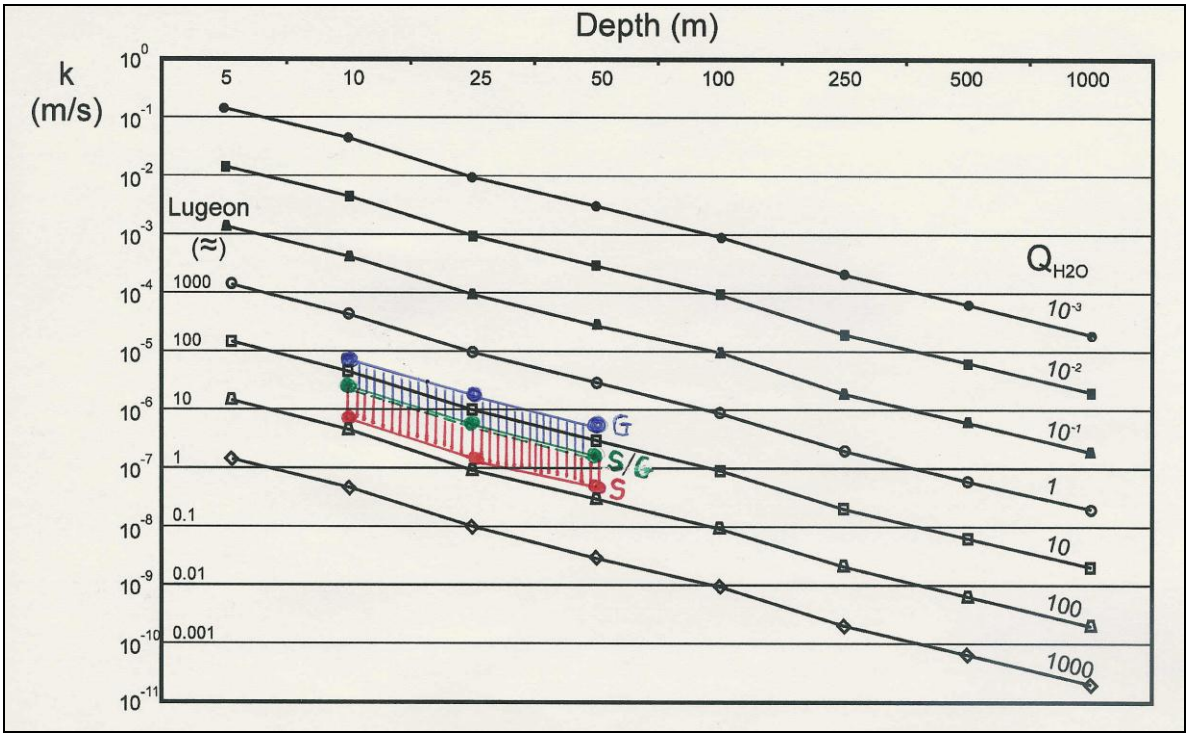

Figure 10 An example of Q_{H2O} and permeability estimation based on more than 1 km of core logging. Independently measured permeabilities ranged from 0.1 to 100 Lugeons, in the depth range 10-50 m. NB&A contract report (2006).

Example of Q_{H2O} estimation

Clay-bearing, well-jointed rock at 100 m depth, with a low assumed JCS of 10 MPa:

Regular Q-value = $\frac{50}{9} \times \frac{1.5}{4} \times \frac{0.66}{1}$ = 1.4, i.e. 'poor'

$$Q_{H_2o} = \frac{50}{9} \times \frac{4}{1.5} \times \frac{0.66}{1} \times \frac{100}{10} = 98$$

K $\approx 10^{-8}$ m/s (at 100 m depth)

(Quite low permeability due to clay coatings, and compressible joint walls, despite the extensively jointed nature of this rock mass).

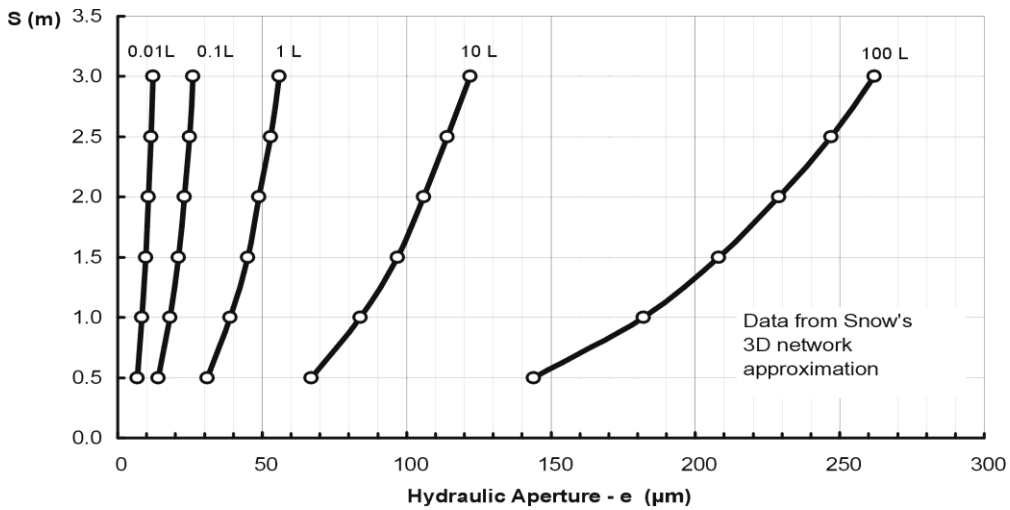

Figure 11 Based on a simplified cubic network model from Snow (1968), it can be shown that K≈10-8 m/s (approx. 0.1 Lugeons), may be composed of (mean) hydraulic apertures (e) of between 15 and 25 µm, for assumed mean conductor spacings of between 0.5 and 3.5 m. Such results suggest the need for high-pressure pre-injection and use of ultrafine cements. Barton (2004).

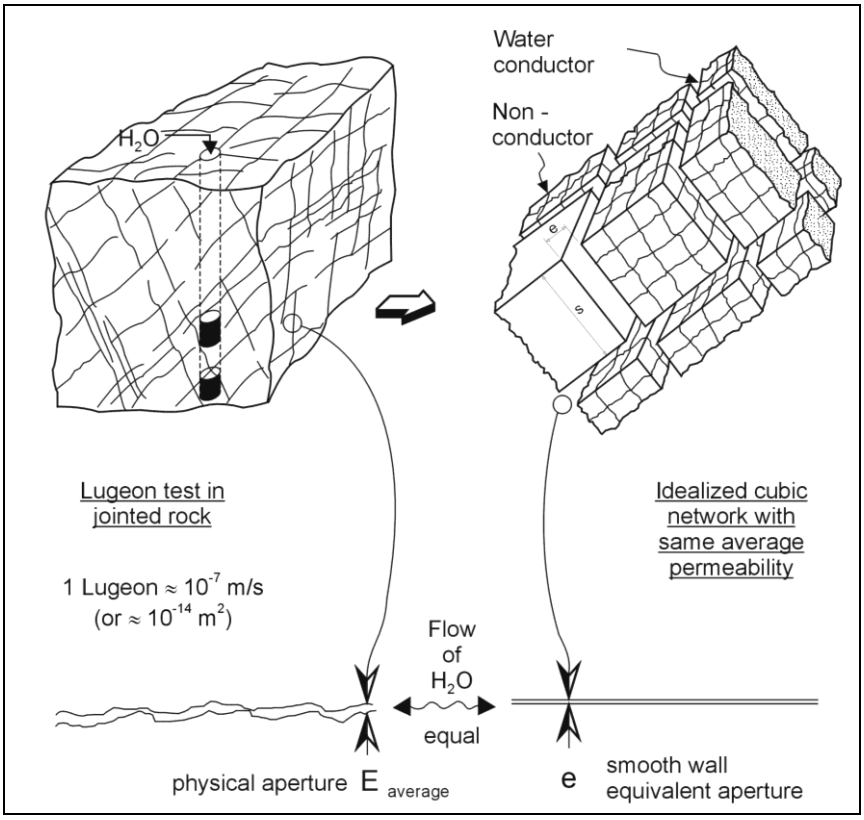

Figure 12 A cubic network approximation to flow and leakage in rock masses ('the engineering approach'). The permeability shown in Figure 11 is based on $k=e^2/12$ for one conductor, $K_1=e^2/12 \times e/S$ for one set, and $K_2=2e^3/12S$ for the rock mass, i.e. two of the three sets controlling flow on average. Snow (1968) with additions by Barton (2004). Note $E \approx \sqrt{(e^2 \times JRC^{2.5})}$ and $E \geq 4d_{95}$ for successful grouting – often requiring grouting pressures of 5 to 10 MPa.

Figure 13 A station cavern showing the need of pre-injection for both water control, and reduction of over-break. Permeability measurement and extrapolation using Q_{H2O} can be used for selecting grouting materials and grouting pressures. When Lugeon values are typically from 10 to 100, less difficulties with pre-injection are expected, but consequences of no pre-injection are greater.

THE BASIC TUNNEL AND CAVERN SUPPORT CHART, Q AND RMR CONVERSION

There is such widespread use of RMR, often in parallel with Q, that it is appropriate to address possible inter-relationship between the two. This of course has been the subject of a lot of publications. One 'camp' utilizes the 'ln' (natural logarithm) format, as in equation 1, in Figure 14, while the other 'camp' utilize the 'log' format, as in equation 2 in this figure. Since the latter format is simpler, and gives a more tangible range of RMR in relation to the Q-scale (avoiding the negative values that occur below Q = 0.01), it has been used by the writer also in relation to stand-up time and deformation modulus conversion between the two systems.

Stand-up time using simple log Q-RMR conversion

While there are admitted pitfalls when attempting to utilize Q to RMR conversion, due to some serious differences in structure and parameter weightings between the two systems, it is nevertheless considered that the advantages may outweigh the disadvantages. For this reason, both stand-up time estimates from Bieniawski (1989), and deformation moduli trends with RMR have been utilized, in an attempt to add to the tools available. Since we are engineers, and not scientists, our craft is the ability to make realistic approximations, leaving all decimal places on the calculator.

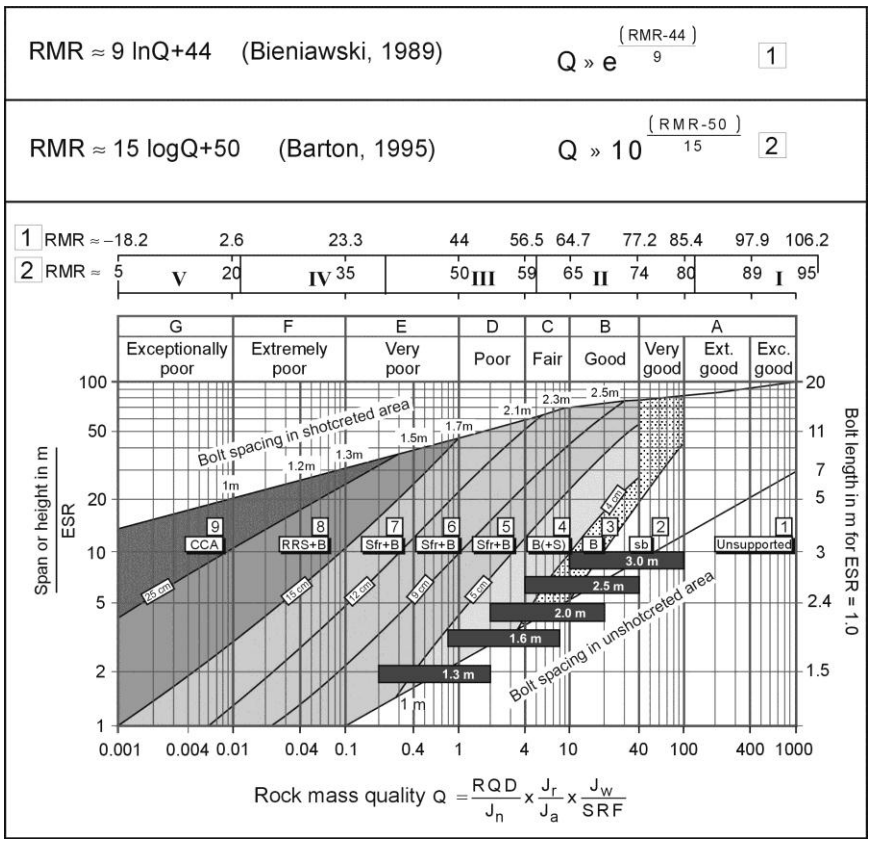

Figure 14 The Q-support chart from the Grimstad and Barton (1993) update for S(fr) in place of S(mr). The black areas referto aspects of TBM tunnel-support, where Q-values are easy to misinterpret due to lack of overbreak (Barton, 2000). The two Q-RMR formulæ refer to the 'standard' Bieniawski (1989) format, and a suggested improvement that is easier to estimate in the field. It also avoids an unwanted negative value of RMR when Q < 0.01.

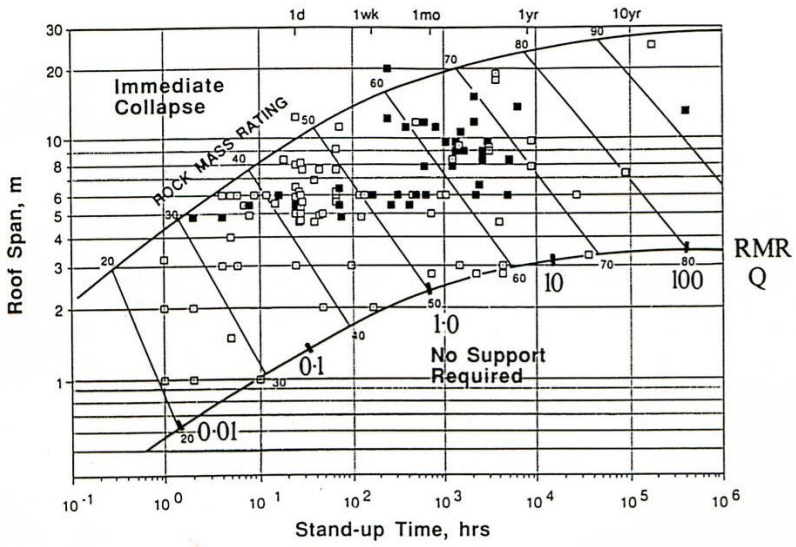

Figure 15 Bieniawski(1989) stand-up time estimations. Note the large Q-value approximations next to the small RMR numbers. The conversion is based on Figure 14 (equation 2).This diagram suggests that when the Q-value is as low as e.g. 0.01, or RMR as low as 20, the stand-up time for a <1m advance may be a matter of minutes, with collapse imminent or immediate if an advance of 2 to 3 m was made – against better judgement, in such poor conditions. Use of spiling combined with rib-reinforced shotcrete RRS arches, and immediate robotic S (fr) application is suggested.

DEFORMATION ESTIMATION BASED ON Q

For many years the writer has assembled information on cavern deformations, cavern size, and Q-values. Barton et al. (1994) showed an updated version, including performance data from various stages of the Gjøvik Olympic cavern excavation. By good fortune, researchers Chen and Guo (1997), followed the same (Q/SPAN) plotting format, and kindly provided the writer with a large set of data from tunnels in Taiwan, driven in significantly poorer rock conditions.

The two sets of widely different deformation data are shown in the left side of Figure 16, with some hand-annotations to emphasise the unexpectedly simple common trend that was discovered when the Taiwan data was added:

$$\Delta\,(\text{mm}) = \text{SPAN}\,(\text{m}) / Q$$

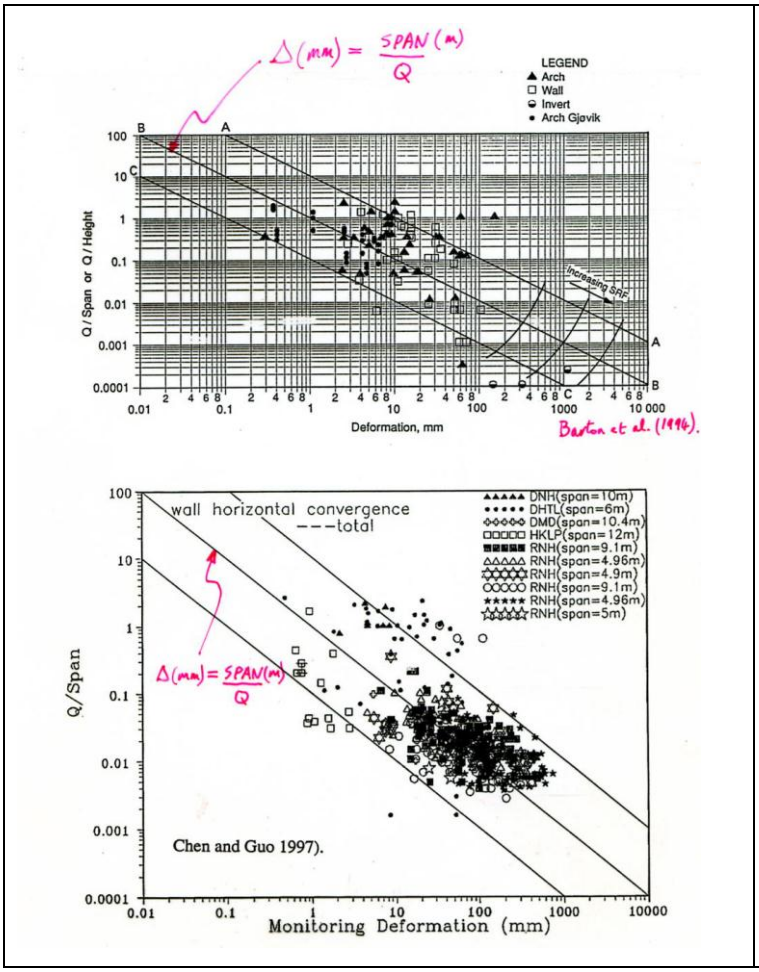

$$\Delta\,(\text{mm}) = \frac{\text{SPAN(m)}}{Q}$$

(central trend of data)

$$\Delta_v \approx \frac{\text{SPAN}}{100.Q}\sqrt{\frac{\sigma_v}{\sigma_c}}$$

$$\Delta_h \approx \frac{\text{HEIGHT}}{100.Q}\sqrt{\frac{\sigma_h}{\sigma_c}}$$

$$Ko \approx \left(\frac{\Delta_h}{\Delta_v}\right)^2\left(\frac{\text{SPAN}}{\text{HEIGHT}}\right)^2$$

Improved empirical links to tunnel or cavern deformation

Figure 16 Q/SPAN versus deformation was a plotting format used by the writer for many years. The top-left figure from Barton et al. (1994) includes some Gjøvik Olympic cavern data concerning pilot tunnels and top headings. The bottom-left figure from a Chinese language article by Chen and Guo (1997), adds hundreds of data from tunnels in Taiwan that showed significant deformation problems. The equations given on the right-side of the figure show the equation of the central trend line, followed by some empirical improvements for reducing scatter, using the ‘competance factor’ principle (i.e. stress/strength). This has a similar role to stress/modulus, but is simpler to estimate.

Example application of the deformation formulæ

Nathpa Jhakri hydropower cavern

SPAN = 20 m, Height = 50 m, representative Q-value = 3,

σ_c= 35 MPa, σ_h = 4 MPa, σ_v = 6 MPa

$\Delta_v = 20{,}000/(100 \times 3) \times (6/35)^{0.5} = 28$ mm (i.e. within range of MPBX measurements in arch)

$\Delta_h = 50{,}000/(100 \times 3) \times (4/35)^{0.5} = 56$ mm (i.e. within range of MPBX measurements in walls)

$K_o = [56/28]^2\ (20{,}000/50{,}000)^2 = 0.64$ (measured $K_o = 4/6 = 0.66$)

RELATING SUPPORT COSTS AND TIME TO Q

Since the Q-system support recommendations appear to be widely used, it may be of interest to present two independent assessments of the extra costs and time involved, when Q-values are low, compared to the 'plateau' where higher Q-values cause minimised support costs and excavation times.

The first example from an NB&A contract, shows the cost estimates for three sizes of tunnel cross-section, using the quantities of arch *and* wall support given by direct application of Q-system-based 'rules' that were published in the 1970's. (See Table 3).The standard support elements were different combinations of B + S(fr), and the quantities were obtained directly from Figure 14 support chart format.

The permanent support recommendations are strictly following NMT support philosophy, i.e. that combinations of B + S(fr) represent permanent support, when inflow of water has been solved by cheaper means than a concrete lining and membrane. Pre-injection, or free-standing bolted PC-elements with outer membrane, are two solutions to avoid having to design to take full water pressure. Dry-but-drained is the key concept. Barton and Grimstad (1994, 2004).

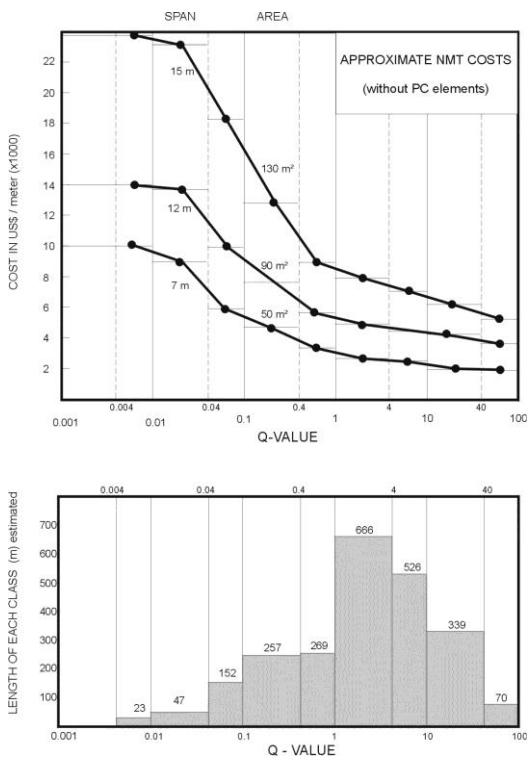

Figure 17 Direct application of Q-system permanent support recommendations in different Q-value ranges, using Norwegian unit prices for B, S(fr), drill-and-blast, mucking and 3 km transport.

In Figure 17, the support costs have a superimposed Q-value statistic based on NB&A logging of numerous boreholes along the tunnel route. The Q-histogram method of collecting and sorting data was used. Total costs for any of the three tunnel alternatives (e.g. ramps, two-lanes, and three-lanes), can be obtained by multiplication of the meters of tunnel of a particular Q-class, and the US $ /m (x 1000) costs.

Table 3 Empirical rules for estimating wall support, and general temporary support.

1.	***Temporary Support***	a) b) c)	increase ESR to 1.5 × ESR increase Q to 5Q (arch) Increase Q_w to $5Q_w$
2.	***Wall Support*** (based on modified quality Q_w for walls)	a) b) c)	select $Q_w = 5Q$ (when $Q > 10$) select $Q_w = 2.5Q$ (when $Q < 10$) select $Q_w = 1.0Q$ (when $Q < 0.1$)

Note 1 Use total excavation height (H) for wall support design.
Note 2 Q is the general rock quality observed when inspecting the arch *or* walls of a tunnel. For local variations of rock quality (arch or walls), map locally and change support as appropriate. (Q_w is *not* the observed value of Q in a cavern wall.)

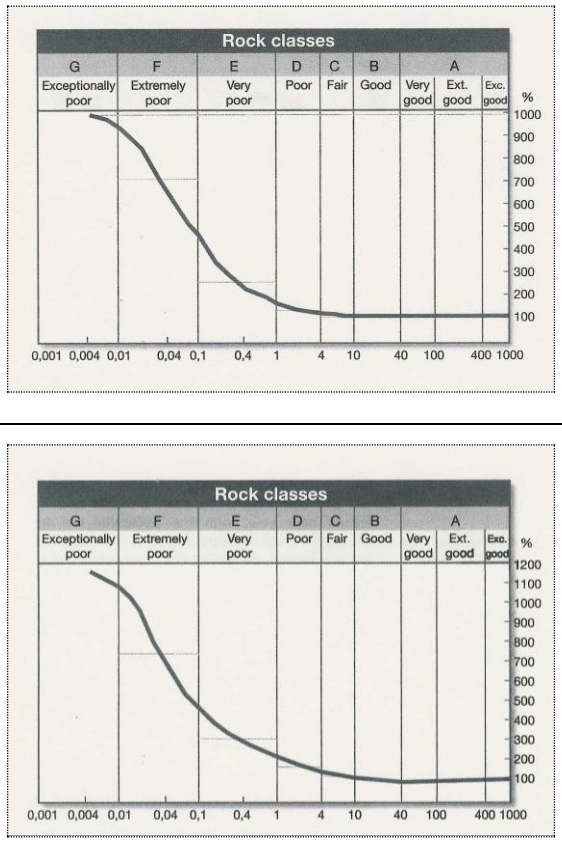

Q = RQD/Jn x Jr/Ja x Jw/SRF

Figure 18 Relative time and cost in relation to Q-values, based on a contractor's calculations for a long 100 m^2 tunnel. These diagrams are useful for arguing the merits of high pressure pre-grouting, which helps to bring the *effective* Q-value down the curve, to the right. Roald et al. (2001). By arguing for small individual improvements in Q-parameter values, it is possible to deduce a 'snowball' increase in effective Q-values as a result of effective pre-grouting. This results in potential increases in seismic velocity, deformation modulus and shear strength, and of course a reduction in permeability. Support needs are reduced: longer rounds can be used.

SOME LESSONS FROM THE GJØVIK OLYMPIC CAVERN INVESTIGATIONS

In the last section of this paper, some of the lessons learned and techniques applied when investigating ground conditions and modelling planned excavation and support of this large cavern will be briefly reviewed. Reference will be made to some of the Q-correlations given earlier in this paper. A start will be made with the comparison of core logging (cross-hatched area: Figure 19) and the Q-logging performed in existing near-by excavations (black area: Figure 19). Note the 'tail' on RQD logged in the case of core, and the lack of a 'tail' logged in existing excavations. This was caused by lack of data where shotcrete covered the poorest rock, when logging existing excavations.

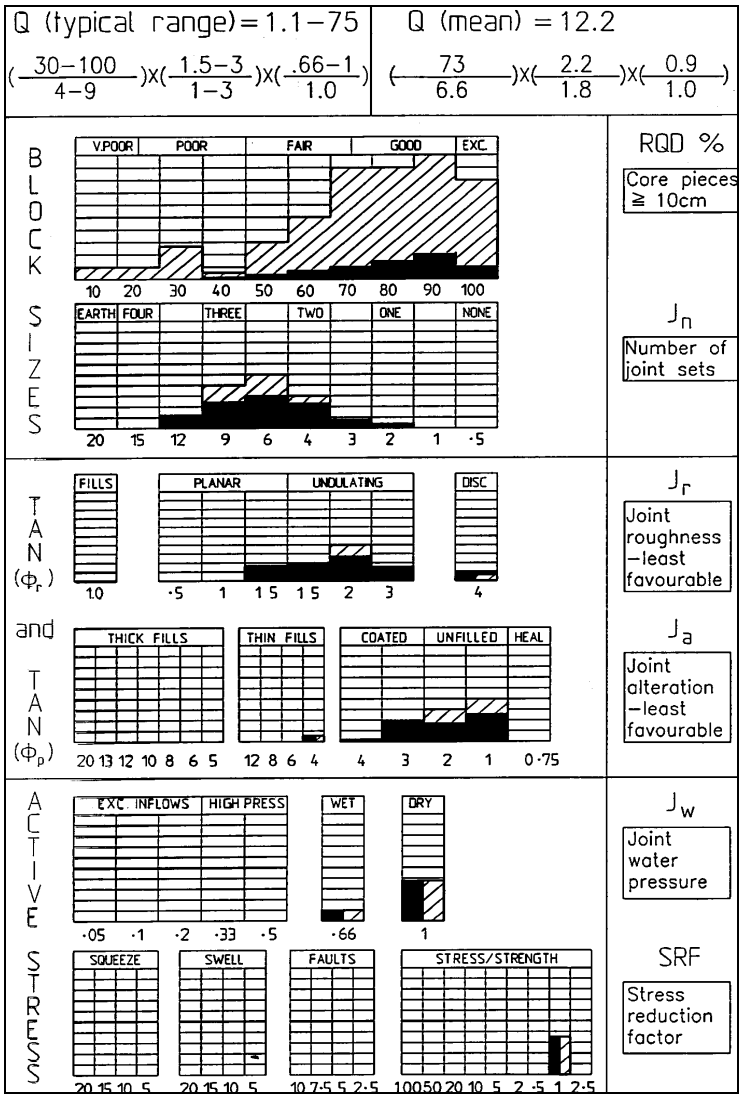

Figure 19 Q-histogram logging of core (4 holes) and existing local excavations, performed by different loggers at different times. Barton et al. (1994).

The boreholes used for core recovery were permeability tested (K mostly ≈ 10^{-7} to 10^{-8} m/s), and were also used for cross-hole seismic tomography. Two examples are shown in Figure 20. The expected increase in velocity with depth, from about 3.5 to 5.0 km/s is shown. What was unexpected was that the rock quality (RQD, F m^{-1}, and Q) did not show a corresponding general increase in quality, as can be ascertained by studying Figure 21, which shows the velocities interpreted close to one of the boreholes.

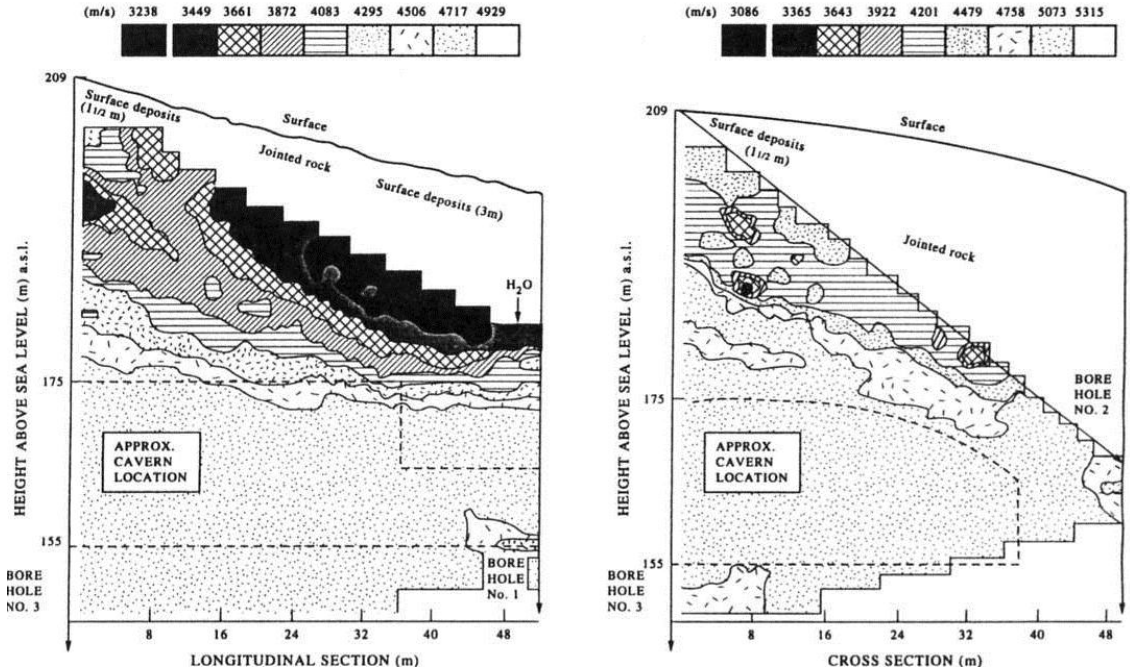

Figure 20 Crosshole seismic tomography between two pairs of holes at the Gjøvik cavern site.

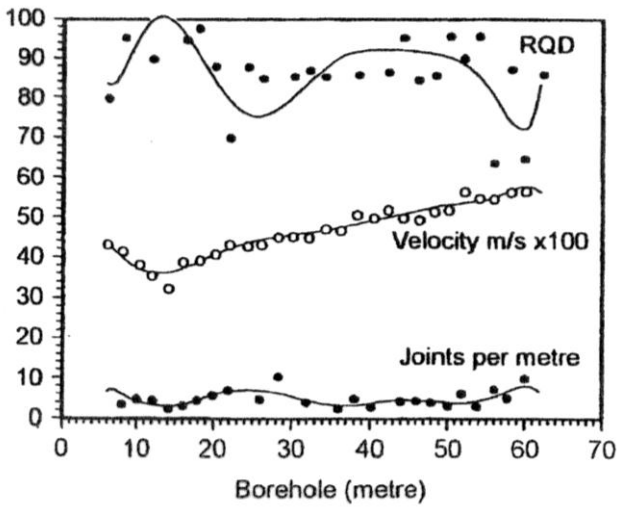

Figure 21 Note lack of a general rock quality improvement with depth, compared with the consistent rise in P-wave velocity. The Q-value logged down the holes mostly varied between 1 and 30, with a mean of 10 to 12, and showed no tendency for improved quality below about 5 m. Barton et al. (1994).

The Q-Vp-depth models shown earlier in Figures 7 and 8 indicate how velocity increase can occur without the need for Q-value increase. However, between 25m and 50 m the predicted increase in velocity is relatively minor, such as 4.5 to 5.0 km/s. The increase of closer to 2 km/s between 10 and 60 m depth suggested in Figure 21, may be explained by a measured or interpreted horizontal stress increase, which was as much as 5 MPa over this same depth range.

This increase, with little assumed change in rock quality, is possible because of the rough state of the conjugate jointing (high Jr and JRC), and due to the relatively sound tectonised gneiss, with UCS about 90 MPa, and JCS about 75 MPa. In softer rock like chalk, ‘acoustic closure’ (in relation to Vp) occurs at much shallower depths than this.

SOME IMPORTANT ASPECTS OF NUMERICAL MODELLING

When confronted with the modelling of a very large cavern, such as Gjøvik's 62 m span, with (arguably) hundreds of thousands of individual interlocked blocks involved, there are those who would prefer to apply continuum FEM, FLAC or PHASES, using the traditional argument that such a large number of blocks 'cannot' be modelled as a discontinuum, and therefore that a much simpler continuum approach can be used.

A glance at the comparison of numerical models performed by an NGI colleague (Figure 22, from Backer, pers. comm.(1998), should be convincing enough to suggest that little may be learned from the continuum models. Besides differences in mode and magnitude of deformations, there are fundamental differences in the stress distributions too, when modelled jointing is actually capable of normal and shear adjustments, as in UDEC-BB, rather than a pseudo-jointing that does not 'disturb' the continuum modelling.

This should be born in mind when the argument proposed for performing the simpler continuum models is that 'at least you get the stress distribution'. You may not in fact get *realistic* stress distributions.

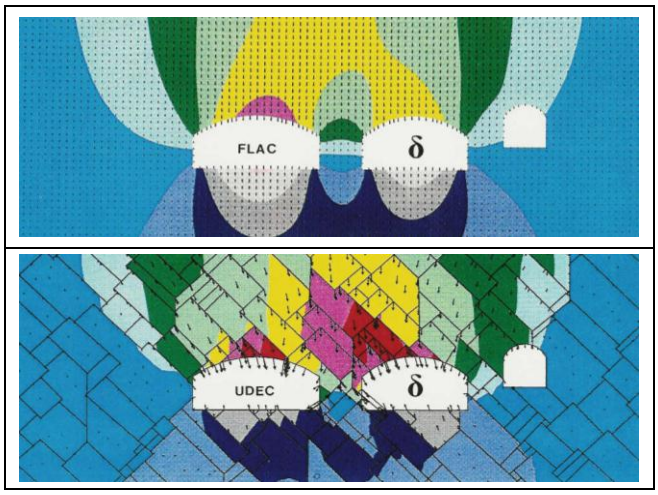

Figure 22 A demonstration of some of the limitations of continuum models as compared to discontinuum models, for showing the potential deformation modes (and support needs) in large tunnels and caverns. Backer, pers. comm.(1998).

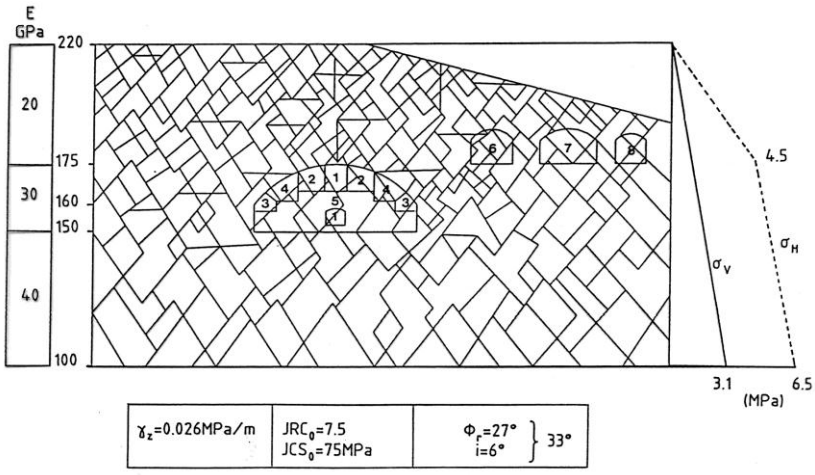

Figure 23 The joint geometry, modulus variation with depth, and BB joint input data used in the UDEC-BB modelling of the Gjøvik Olympic cavern. Physical modelling had earlier shown the possibility of ground heave ('negative' vertical deformation) with similar high levels of horizontal stress. Upwards or downwards deformation depended on the joint pattern. The modelled 7 to 9 mm downwards directed deformation matched the unknown measured result almost perfectly. Barton et al. (1994).

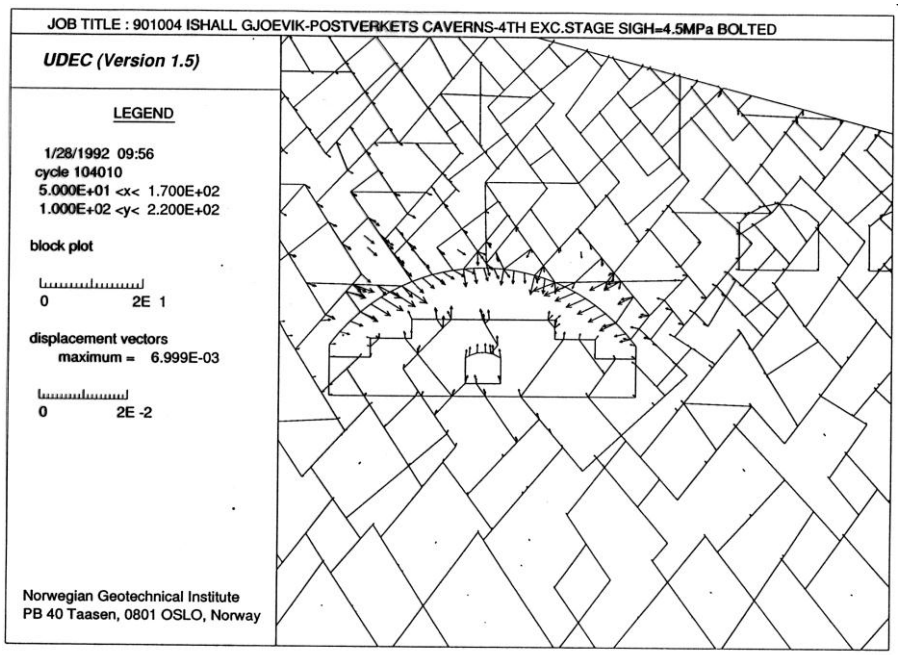

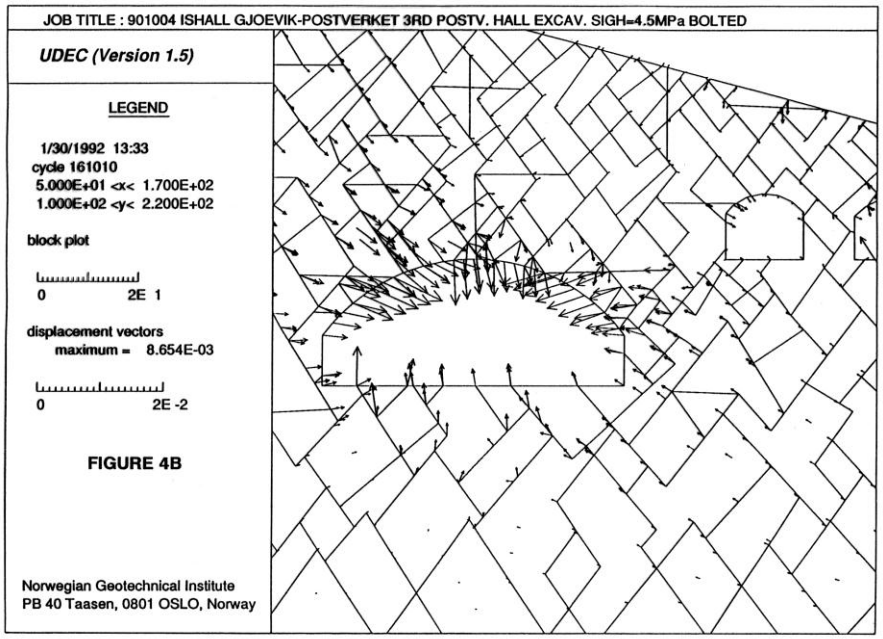

Figure 24 Two stages of the multiple excavations at Gjøvik, which included final excavation of adjacent Postal Service caverns, which caused some subtle changes to the main cavern. Note the maximum modeled deformations of 7.0 and 8.7 mm for the huge (62 m span) ‘top heading’ and final stages, when the total height was 24 m. UDEC-BB modeling by Chryssanthakis, of NGI. Barton et al. (1994).

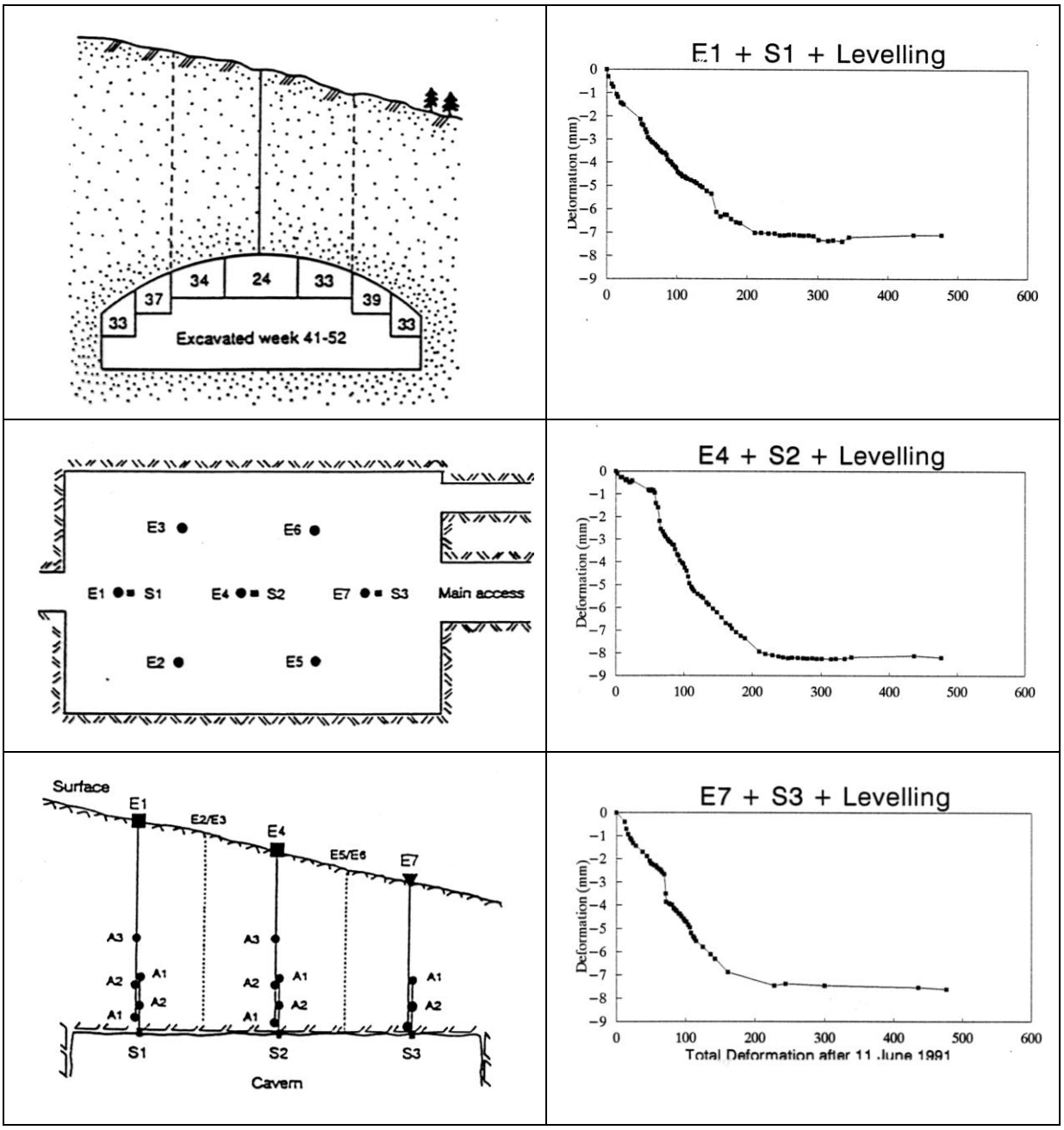

Figure 25 Three views of the cavern that show the location of the ten MPBX. On the right-hand side are the first 500 days of monitoring, obtained by adding the surface leveling to the 'dilation' of the 'E' (external) and 'S' (short internal) extensometers. Maximum measured deformations of 7 to 8 mm were an excellent validation of the class A (blind) modeling with UDEC-BB (7 to 9 mm), and were also a form of validation of BB input data. Key components of the rock mass for stable conditions being achieved with 'normal' NMT Q-based rock support, were the roughness of the jointing, and the fairly high horizontal stress (see Figure 23). Joint roughness was typically Jr = 2, and JRC_o = 7.5, with larger scale undulation that was assumed to give a 'Patton i-value' of 6º.

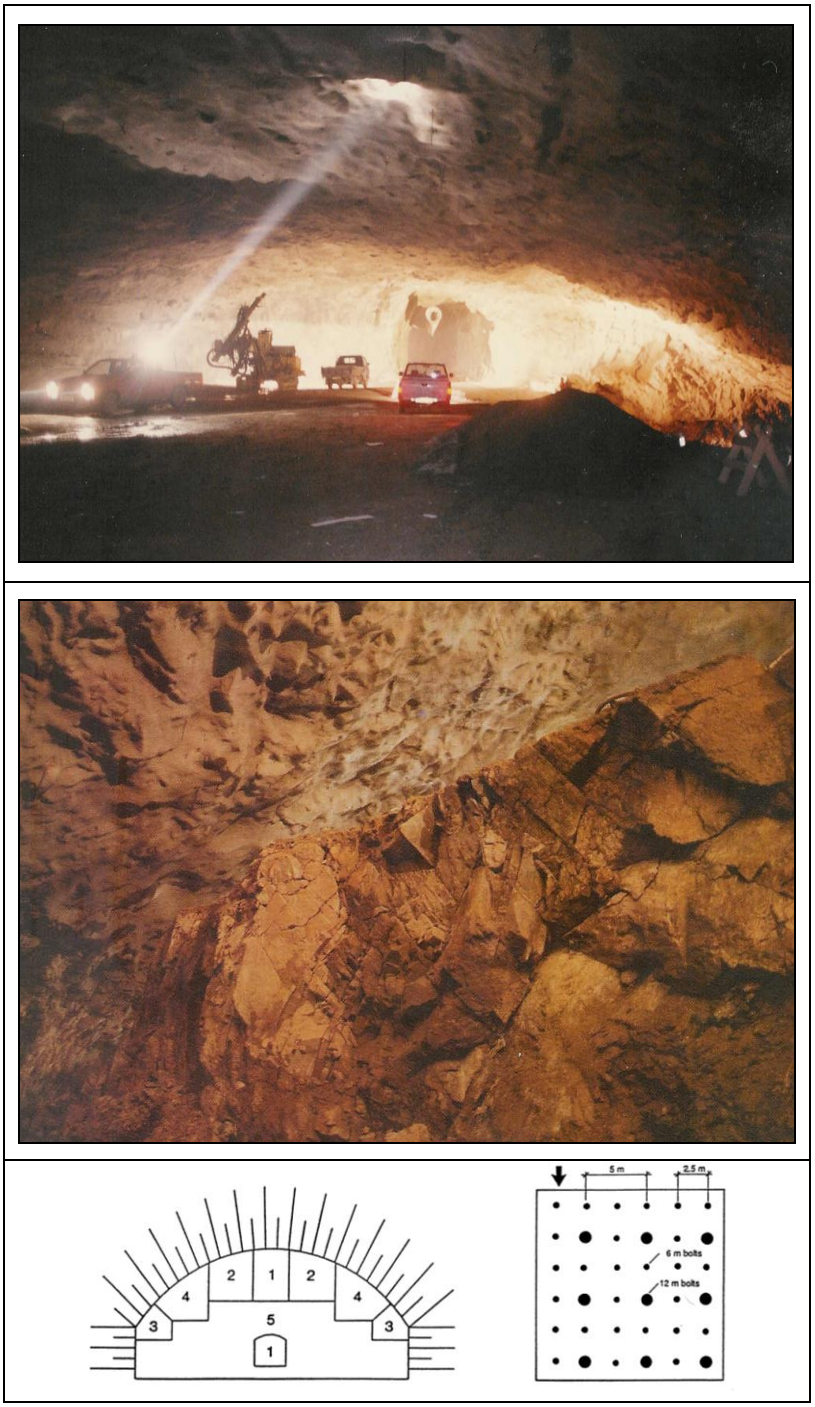

Figure 26 Views of the top-heading shown in Figures 24a and 25a. Note the conjugate jointing in the gneiss, which was responsible for more than 1.5 m overbreak in places in the arch, some 20 m above this lower photo, which was taken from the floor of Level 3. The NMT permanent support was S(fr) 10 cm (a mean 9.8 cm from numerous control borings), plus the bolting and light cable (2 x 16 mm twin-strand) depicted in the lower diagram. The 140,000 m^3 (62 x 24 x 120 m) cavern was excavated and supported in roughly 7 months. (See week-numbers and excavation stages in Figure 25a).

A CRITICAL DISCUSSION OF INPUT DATA FOR CONTINUUM MODELLING

A long time ago, in the late 1960's, there was a move in some rock mechanics circles to try to move beyond the confines of continuum modeling, and focus on the possible effects of jointing on the performance and reinforcement needs of rock excavations, be they tunnels, slopes or dam abutments.

Thanks to the late 1960's modeling developments of Goodman and his colleagues with joint elements in FEM codes, followed by Cundall in the early 1970's, first with μDEC, then UDEC and later with 3DEC, this focus could be fulfilled by an increasing number of rock mechanics practitioners around the world. However, utilizing these codes correctly, with realistic input data, needs experience, time and therefore budgets to match.

Presumably as a result of time and budgetary pressures, and also the developing need to model large-scale mining problems, there has been a marked 'backwards' movement into the use of convenient continuum codes, which also have particularly good graphics presentation. Simple software packages for handling the unjustifiably complex input data calculations (e.g. Figure 27) are also provided, so that a smart user might theoretically need only limited understanding of rock mechanics principles to use the codes 'successfully'.

$E_m\ (\text{GPa}) = \left(1-\frac{D}{2}\right)\sqrt{\frac{\sigma_{ci}}{100}} \times 10^{(GSI-10)/40}$	$E_m \approx 10 \times Q_c^{1/3}$
$\sigma'_{cm} = \sigma_{ci} \times \frac{(m_b + 4s - a(m_b - 8s))(m_b/4 + s)^{a-1}}{2(1+a)(2+a)}$	$\sigma_{cm} \approx 5\gamma\, Q_c^{1/3}$
$\phi' = a\sin\left[\frac{6am_b\left(s + m_b\sigma'_{3n}\right)^{a-1}}{2(1+a)(2+a) + 6am_b\left(s + m_b\sigma'_{3n}\right)^{a-1}}\right]$	$"\phi" \approx \tan^{-1}\left(\frac{J_r}{J_a} \times \frac{J_w}{1}\right)$
$c' = \frac{\sigma_{ci}\left[(1+2a)s + (1-a)m_b\sigma'_{3n}\right]\left(s + m_b\sigma'_{3n}\right)^{a-1}}{(1+u)(2+a)\sqrt{1 + \left(6am_b\left(s + m_b\sigma'_{3n}\right)^{a-1}\right)/((1+a)(2+a))}}$	$"c" \approx \left(\frac{RQD}{J_n} \times \frac{1}{SRF} \times \frac{\sigma_c}{100}\right)$

Figure 27 The extraordinarily complex formulæ (left), for developing input data for some recent continuum models, and comparison to some of the less developed, and equivalent Q-based formulæ. For a non-mathmatician, in other words for a simple rock engineer, there is no possibility to have any feel for the influence of local rock quality on the rock mass compression strength, friction angle or cohesion, when formulations require software, rather than estimation for their evaluation.

The writer has often used the 'Chinese method' of rapidly thumbing from the back of a consultant's report to the front, whereby the coloured appendices of endless stress distributions and deformation patterns, can be read almost as in a film. Does all this 'colour' represent anything real? Would the numerical modelers know how to input a neglected clay seam – without 'smoothing-it-out' in a continuum approximation? Would equations c) and d)

for φ' and c' in Figure 27 change very much?

An additional problem is that the failure mode involved in rock breakage is actually highly unlikely to be governed by the Mohr-Coulomb style of strength criterion ‘c + tan φ’, because rock fails at small strain, breaking the cohesion, followed by mobilization of friction at larger strain. It is for this reason that continuum models with such strength criteria (i.e. with the ‘+’ term) make such a remarkably poor job in modelling actual rock failure, as documented in careful experiments. This important fact was emphasised by Martin et al. (2002). The obviously poor performance is shown in Figure 28.

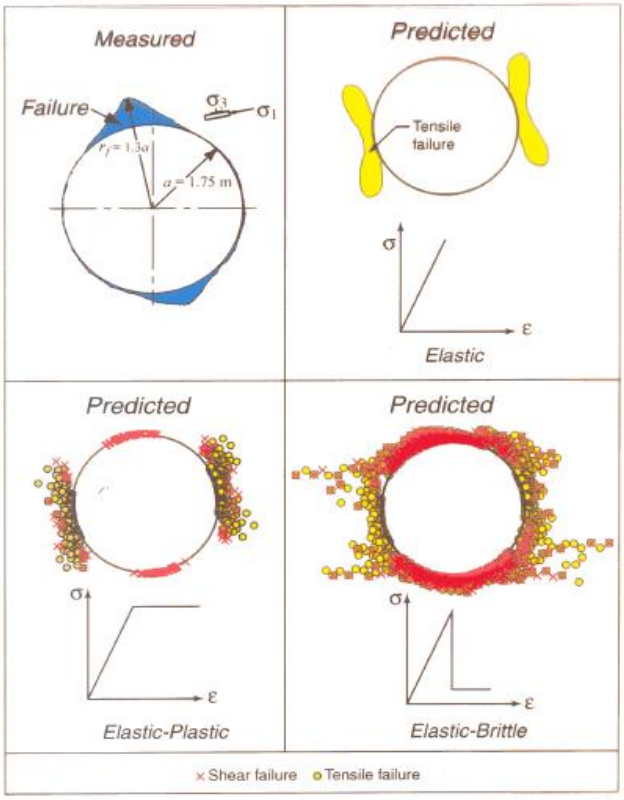

Figure 28 Attempts to model the rock breakage observed in a line-drilled tunnel at the URL in Canada, using continuum models having strength criteria of the form ‘c + tan φ’, when the actual breakage is by a process similar to ‘c *then* tan φ’, due to cohesive failure at small strain followed by frictional mobilization at larger strain. Martin et al. (2002).

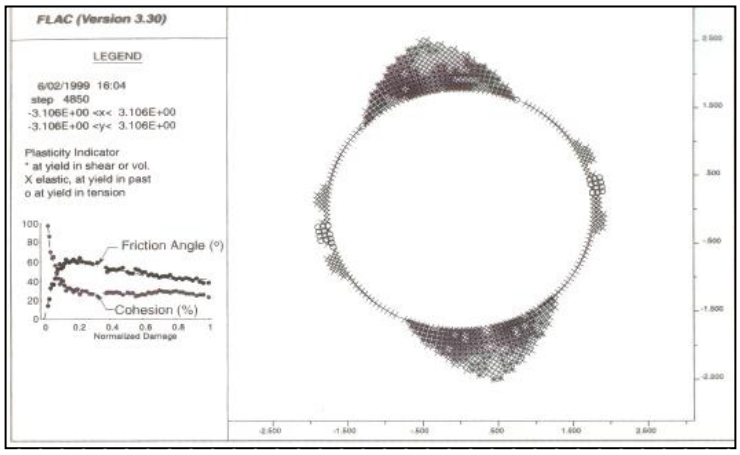

Figure 29 Degradation of cohesion at small-strain, and simultaneous mobilization of friction by means of a ‘manual’ entry into a FLAC calculation by Diederich, (Martin et al. 2002), shows excellent matching to the URL break-out position and depth. A more valid fracture mechanics approach may perhaps be achieved by FRACOD. (Shen)

In Figure 27, simple Q-based equations for 'c' and 'φ' were shown, that are actually found to be composed of each 'half' of the Q_c-formulation. They have the advantage of not requiring software for their calculation – they already exist in the Q-parameter logging data. We define them as follows:

'cohesive component' CC = RQD/Jn x 1/SRF x σ_c/100

'frictional component' FC = $\tan^{-1}$[Jr/Ja x Jw]

RQD	J_n	J_r	J_a	J_w	SRF	Q	σ_c	Q_c	*FC°*	*CC* MPa	V_p km/s	E_{mass} GPa
100	2	2	1	1	1	100	100	100	63°	50	5.5	46
90	9	1	1	1	1	10	100	10	45°	10	4.5	22
60	12	1.5	2	0.66	1	2.5	50	1.2	26°	2.5	3.6	10.7
30	15	1	4	0.66	2.5	0.13	33	0.04	9°	0.26	2.1	3.5
10	20	1	6	0.5	5	0.008	10	0.0008	5°	0.01	0.4	0.9

Figure 30 Five hypothetical rock masses with reducing quality from top to bottom of the tabulation. Note the difference between Q and Q_c due to normalization by σ_c/100. The P-wave velocity and (pseudo-static) deformation modulus estimates are from the central diagonal, near-surface (25 m depth) inter-relationships given in Figure 7. Barton (2002).

Plate loading tests taken to such high stress levels that rock mass failure occurs are rare. The measurement of P-wave velocity at such sites may allow tentative extrapolation to other sites through a common rock mass quality estimate. Such data can then be a source of tentative rock mass strength ($\sigma_{c\ mass}$) estimation. The small table below suggests compressive (and cohesive) strengths in rock masses somewhat different to those usually assumed. They also show some implicit variation from the values set up in Figure 29 (from specific Q-parameter combinations), but reinforce the idea of potentially very high cohesive strengths (e.g.10's of MPa) in competent rock masses.

Table 4 Plate load tests driven to failure, with corresponding velocity and modulus data for the different rock masses. Savich et al. (1974).

Velocity V_p (km/s)	2.3	3.7	4.0
Modulus E_{mass} (GPa)	1	3	15
Rock mass σ_{cm} (MPa)	4	20	50

Figure 31 Examples of rock masses with particularly low CC (left), and particularly low FC (right). These require relatively more shotcrete (left) and relatively more bolting (right). The original Q-system case records have apparently reflected these different needs, and the Q-parameter ratings developed have given the possibility of realistic CC and FC values.

CONCLUSIONS

1. Q-system linkages to parameters useful for design are based on sound, simple empiricism, that works because it reflects practice, and that can be used because it can be remembered. It does not require black-box software evaluation.

2. The wide range of Q-values (0.001 to 1000) reflects to some degree the very wide range of geological conditions, and is probably responsible for the fact that empirical equations based on the Q-value are particularly simple.

3. An integration of Q with seismic data is useful because there is a limit to how many boreholes can be drilled, how many cores can be logged, and how many permeability tests can be performed. The ability to extrapolate these 'point sources' of information helps to project rock quality classes along a tunnel, or to different parts of a large cavern.

4. Due to the effect of increased stress at greater tunnel or cavern depth, it must be expected that deformation modulus and seismic velocity will increase. Eventual sonic logging or cross-hole tomography ahead of a tunnel face may therefore give a higher velocity than the rock quality may suggest.

5. The most simple and least accurate approximation for permeability is that the number of Lugeon: $L \approx 1/Q_c$. This is strictly for the case of clay-free, jointed, low porosity rock masses. A more generally applicable approximation uses an inverted Ja/Jr term and 100/JCS to give a better link to permeability. A high value of Q_{H2O} implies low permeability, and a general reduction of permeability with depth is also modelled.

6. There are other surprisingly simple relationships that have their origin in empirical links to Q-values. Support pressure appears to be inversely proportional to deformation modulus, and a central trend for tunnel deformation is that Δ in millimetres is equal to span in meters divided by Q. An improved fit to the quite scattered deformation data incorporates the stress-to-strength ratio, with differentiation of vertical and horizontal stress, for estimating arch or wall deformation.

7. As expected from a system that has it's origin in tunnel and cavern support selection, there is a strong correlation of time for construction with Q, and cost of construction with Q. The strongest correlation, where the curves of time and cost are steepest, is where the Q-value is between 0.01 and 1.0. It is here that the greatest benefit of high pressure pre-injection may be obtained, with effective, apparent improvements in many of the Q-parameters, and therefore in correlated properties like increased velocity and modulus, reduced support needs, and increased round lengths.

8. Application of discontinuum codes like UDEC-BB gives much more understanding and more relevant behaviour predictions than continuum codes. The example of the Gjøvik Olympic cavern of 62 m span is given, where the blind prediction of displacements was remarkably accurate, despite the possibility of either upward or downward displacements, that depended upon the interaction of joint orientations, their strength and stiffness, and horizontal stress levels.

9. Strength criteria of the form 'c + tan φ' used in continuum codes, which have remarkable complexity requiring software for evaluation of their components, have in addition the problem that when supposedly simulating shear failure, the reality is cohesion reduction at small strain, and friction mobilization at larger strain. Mohr-Coulomb and Hoek-Brown strength criteria may therefore need to be of the form 'c *then* tan φ'.

REFERENCES

Barton, N., Lien, R. & Lunde, J. (1974). Engineering classification of rock masses for the design of tunnel support. *Rock Mechanics.* 6: 4: 189-236.

Barton, N., By, T.L., Chryssanthakis, P., Tunbridge, L., Kristiansen, J., Løset, F., Bhasin, R.K., Westerdahl, H. & Vik, G.. (1994). Predicted and measured performance of the 62m span Norwegian Olympic Ice Hockey Cavern at Gjøvik. *Int. J. Rock Mech, Min. Sci. & Geomech. Abstr.* 31:6: 617-641. Pergamon.

Barton, N. (1995). The influence of joint properties in modelling jointed rock masses. Keynote Lecture, *8th ISRM Congress*, Tokyo, 3: 1023-1032, Balkema, Rotterdam.

Barton, N. & Grimstad, E. (1994). The Q-system following twenty years of application in NMT support selection. 43rd *Geomechanic Colloquy,* Salzburg. Felsbau, 6/94, 428-436.

Barton, N. (2000). *TBM tunnelling in jointed and faulted rock.* 173p. Balkema, Rotterdam.

Barton, N. (2002). Some new Q-value correlations to assist in site characterization and tunnel design. *Int. J. Rock Mech. & Min. Sci.* Vol. 39/2:185-216..

Barton, N. (2004). The theory behind high pressure grouting. *Tunnels & Tunnelling International*, Sept., 28-30, Oct., 33-35.

Barton, N. (2006). *Rock quality, seismic velocity, attenuation and anisotropy*. Textbook, in press. Taylor & Francis, The Netherlands, 800p.

Bieniawski, Z.T. (1989). *Engineering rock mass classifications: A complete manual for engineers and geologists in mining, civil and petroleum engineering*. 251 p. J. Wiley.

Grimstad, E. & Barton, N. (1993). Updating of the Q-System for NMT. *Proceedings of the International Symposium on Sprayed Concrete - Modern Use of Wet Mix Sprayed Concrete for Underground Support,* Fagernes.(Eds Kompen, Opsahl and Berg. Norwegian Concrete Association, Oslo.

Martin, D.C., Christiansson, R. & Soderhall,J. (2002). Rock stability considerations for siting and constructing a KBS-3 repository, based on experience from Åspö HRL, AECL's HRL, tunnelling and mining. SKB (Swedish Nuclear Fuel Co.), Stockholm, TR-01-38.

Roald, S., Barton, N. & Nomeland, T. (2001). Grouting – the third leg of underground construction. *Norwegian Tunnelling Society,* Publ. Nr. 12.

Savich, A.I., Koptev, V.I. & Zamakhaiev, A.M. (1974). In situ ultrasonic investigation of failure of limestone. *International Society for Rock Mechanics. International Congress,* 3. Denver 1974. *Proc. 3rd ISRM Congress, Denver. IIA:* 418-423. Washington D.C.: National Academy of Sciences.

Sjøgren, B., Øfsthus, A. & Sandberg, J. (1979). Seismic classification of rock mass qualities. *Geophys. Prospect., 27:* 409-442.

Snow, D.T. (1968). Rock fracture spacings, openings, and porosities. *J. of Soil Mech. and Found. Div.,* Proc. ASCE, SMI. 73-91.